GENOMIC AND TRANSCRIPTOMIC PROFILING REVEALS NOVEL BIOMARKERS IN PEDIATRIC ACUTE LYMPHOBLASTIC LEUKEMIA

Ph.D. thesis

Borbála Péterffy, MD

Semmelweis University Doctoral School

Pathological and Oncological Division

Supervisor: Donát Alpár, PhD

Official reviewers: Tibor Szarvas, PhD

Károly Szuhai, MD, PhD

Head of the Complex Examination Committee:

Attila Tordai MD, DSc

Members of the Complex Examination Committee:

Péter Attila Király, MD, PhD

Zoltán Wiener, MD, PhD

Budapest, 2025

1. INTRODUCTION:

Acute lymphoblastic leukemia (ALL) is the most common form of cancer in children, accounting for a significant burden in pediatric oncology. In Hungary, approximately 60-70 children are diagnosed every year. Despite advancements in treatment strategies, challenges persist, particularly in managing disease progression, relapse, and leukemic infiltration of the central nervous system (CNS).

Relapse is the primary reason for treatment failure in pediatric ALL, and it is often linked to the emergence or enrichment of certain genetic alterations harbored by the leukemic blasts.

Leukemic involvement of the central nervous system (CNS) is another significant concern. CNS leukemia (CNSL) is still underdiagnosed in ALL, and meningeal relapse is a common cause of therapy failure. The lack of sensitive diagnostic tools and biomarkers for interrogating the cerebrospinal fluid (CSF) is a major hurdle, preventing the precise identification of patients with clinically significant CNS involvement and a high risk of relapse in the CNS. Cell-based CSF diagnostic methods have limitations, as they are not suitable for detecting blasts that are attached to the meninges, thus CNS manifestation may commonly remain hidden. Novel approaches, focusing on the cell-free fraction of the CSF, such as analyzing circulating tumor DNA (ctDNA) and microRNAs, may offer improved disease detection and monitoring.

To address these challenges, ongoing research aims to integrate advanced molecular techniques into clinical diagnostics. This includes identifying prognostic biomarkers and developing more sensitive methods for detecting CNS involvement, which could enhance risk-adapted therapy selection and improve patient outcomes. Early identification of molecular aberrations contributing to disease progression can aid relapse prediction,

inform therapy adjustment, and even guide targeted treatment against relapse-prone leukemic cell populations.

2. OBJECTIVES:

In my PhD work, we aimed:

- To interrogate the genomic and transcriptomic landscape of Hungarian children with ALL.
- To develop a targeted next generation sequencing (NGS) panel, specifically for the detection of mutations with clinical significance in ALL.
- To identify genetic alterations with therapeutic and/or prognostic relevance.
- To compare the landscape of genetic alterations in matching samples obtained at the time of diagnosis and relapse.
- To investigate miR-181a-5p as a potential biomarker for the diagnosis and monitoring of leukemic infiltration in the CNS.
- To investigate the associations between genetic alterations of the leukemic blasts, miR-181a expression and CNS involvement.
- To assess the diagnostic value and feasibility of miR-181a quantification by droplet digital PCR in CNSL diagnostics.

3. METHODS

Blast-rich samples collected at the time of diagnosis from 150 B-cell precursor ALL (B-ALL), 3 B-cell precursor lymphoblastic lymphoma (B-LBL), 30 T-cell precursor ALL (T-ALL) and 9 T-cell precursor lymphoblastic lymphoma (T-LBL) patients with a mean blast percentage of 78.4% were investigated. Risk stratification and treatment selection were based on ALL IC-BFM 2002, ALL IC-BFM 2009, I-BFM NHL LL 2009, LBL 2018 and Interfant-06 protocols. Follow-up time ranged from 0 to 135 months, with an average of 29 months. Additionally, paired samples drawn at the time of diagnosis and

relapse were analyzed from 19 patients. Measurable residual disease (MRD) assessment on days 15, 33 and 78 of therapy was performed on bone marrow samples using flow cytometry (FCM). Copy number alterations (CNA) were analyzed by multiplex ligation-dependent probe amplification (MLPA) using the P335, P383 and P202 probemixes (MRC Holland). digitalMLPA reactions were performed using an in-development version of the D007 ALL probemix (version D007-X7, MRC Holland). Reactions were carried out according to previously published protocols. Mutational screening was performed using QIASeq Targeted DNA Custom Panel (Qiagen) covering 102 disease-relevant genes frequently (>2%) altered in ALL. Gene-fusions were identified by TruSight RNA Pan-Cancer Panel (Illumina) investigating 1,385 genes, relevant in various malignancies. NGS libraries were pooled and sequenced on a MiSeq platform (Illumina).

For the investigation of CNSL, diagnostic bone marrow (BM) and CSF samples of 35 children with B-ALL (n=28) or T-ALL/LBL (n=7) were collected and analyzed. Serial follow-up CSF samples were collected on day 15, day 33 and around day 100 of treatment. Altogether, 92 CSF samples and 36 BM samples were analyzed. Conventional cell counting, microscopic cytology, and FCM were performed for analyzing the cell fraction of the CSF samples following the ALL IC-BFM protocols. MicroRNA (miR) was isolated from 200 µl of CSF samples (miRNeasy Serum/Plasma Kit, Qiagen, Hilden, Germany), and copy numbers of miR-181a, miR-532 and miR-16 were measured by digital droplet PCR (QX200 System, Bio-Rad). Hierarchical clustering, multiple regression and ANOVA were used to assess the association of normalized microRNA copy numbers and mutation data identified from diagnostic bone marrow samples with the degree of CNS involvement.

4. RESULTS

4.1 Genetic aberrations unveiled by comprehensive profiling

Targeted mutation screening revealed a higher number of aberrations in T-ALL/LBL patients (B-ALL/LBL: 1.5±1.4 vs T-ALL/LBL: 2.7±2.2; $p<0.001$). In B-ALL, variants most frequently affected RAS-pathway genes (*KRAS* (18.5%), *NRAS* (17.8%), *FLT3* (10.3%), while *NOTCH1* (58.6%), *PHF6* (27.6%), *PTEN* (17.2%) and *WT1* (17.2%) were the most commonly altered genes in T-ALL. In total, 175 variants, not previously reported in public databases, were identified, in addition to well-known mutations hotspots and rare, but formerly reported alterations. For instance, *ZEB2* p.Q1072 (2.7%) and *IKZF1* p.N159Y (1.4%), with presumptive prognostic relevance, were uncovered. Three out of six identified *TP53* mutations emerged in the p.R282 hotspot, one of which has not been reported previously. All detected *TP53* variants affected regions coding the DNA binding domain. Variants affecting potentially targetable genes, e.g. *NRAS, KRAS, FLT3, JAK2, IL7R, PTPN11, NF1* and *CRLF2* were observed in 35.6% of high-risk and 29.8% of standard/ intermediate-risk patients (according to ALL IC-BFM 2009 protocol), with a VAF >10%.

MLPA revealed copy number alterations in 55.5% of B-ALL and 66.7% of T-ALL patients. In B-ALL, *CDKN2B* (20.5%), *CDKN2A* (19.9%), *PAX5* (16.4%) and *ETV6* (16.4%) genes were most frequently affected by deletions. *IKZF1* deletion was present in 15.8% of B-ALL patients, while seven of them displayed the *IKZF1*plus (4.8%) genotype. Most commonly identified alterations in T-ALL involved *CDKN2A* (56.7%), *CDKN2B* (53.3%) and *MTAP* (30.0%) deletions, indicating the prevalent deletion of the 9p21 region in this subset of patients. In 30 patients (24 B-ALL, 6 T-ALL), digitalMLPA unveiled CNAs in areas not covered by MLPA probemixes. This more

comprehensive method identified CNAs in 95.6% of B-ALL and 91.7% of T-ALL patients. On average, 12.6 CNAs were identified per patient (mean subchromosomal alteration: 10.6, mean whole chromosome gain/loss: 2.0).

Targeted RNA sequencing revealed gene fusions in 34.9% of B-ALL and 46.4% of T-ALL patients. The most common changes found were *ETV6::RUNX1*, *P2RY8::CRLF2*, and *TCF3::PBX1* in B-ALL, *STIL::TAL1* in T-ALL. Rearrangements involving *ABL1, ABL2, CRLF2, EPOR* and *JAK2* genes with a variety of different partner genes, indicated *BCR::ABL1*-like phenotype in 7.7% (13/169) of B-ALL patients. Additionally, rare fusions including *DUX4* (n=2), *MEF2D* (n=1), *NUTM1* (n=1) and *ZNF384* (n=1) genes were also discovered. Novel chimeric fusions affecting the *JAK2*, *KMT2A, PAX5, RUNX1*, and *NOTCH1* genes were identified in 5 patients. Genes affected by mutations, deletions, amplifications or gene fusions in at least three patients, are depicted in Figure 1.

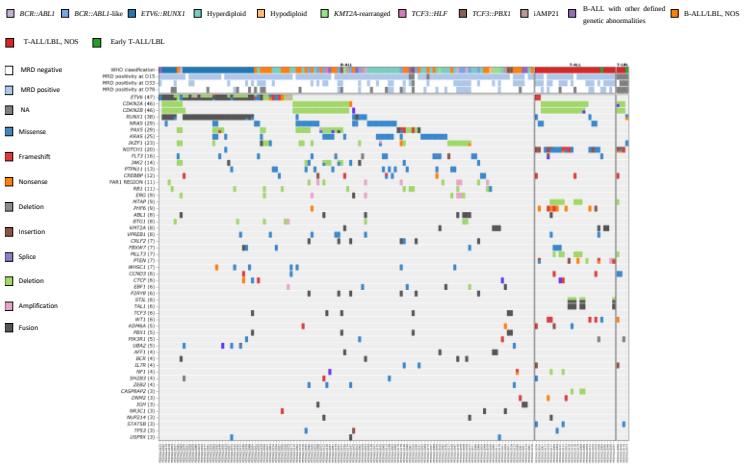

Figure 1. Short somatic variations, CNAs and gene fusions identified in diagnostic samples of 165 pediatric ALL/LBL patients by deep targeted DNA sequencing, RNA sequencing,

and MLPA. Immunophenotype, WHO classification, and MRD status on days 15, 33, and 78 of therapy are also indicated.

4.2 Co-segregation of molecular alterations

Frequent co-occurrence of *KRAS* mutations with *NRAS, BRAF, FLT3* and *CREBBP* mutations were observed in B-ALL (Figure 2.A), while in T-ALL the association of *STAT5B* mutations with *JAK1* mutations, or *NOTCH1* mutations with *PHF6* mutations were uncovered (Figure 2.B). These findings suggest that recurrent clonal selection mechanisms commonly converge on the same or interconnected pathways in individual patients. The frequency of RAS pathway mutations (67.5%), such as *NRAS*, *KRAS, PTPN11,* and *FLT3* mutations were prominent in patients with hyperdiploidy. *UBA2* mutations (85.7%) and *ETV6* deletion (66.7%) occurred primarily in the *ETV6::RUNX1* subgroup. All except for one patient with *BCR::ABL1* fusion carried *IKZF1* deletion, while in *BCR::ABL1*-like patients, *IKZF1, EBF1, PAX5* and PAR1 deletions, as well as *JAK2* and *ZEB2* mutations were enriched. In addition to the numerous concurrent deletions of genes located in chromosome region 9p21, several positive associations between *NOTCH1, PHF6, WT1, FBXW7, MLLT3* and *MTAP* alterations were present in T-ALL.

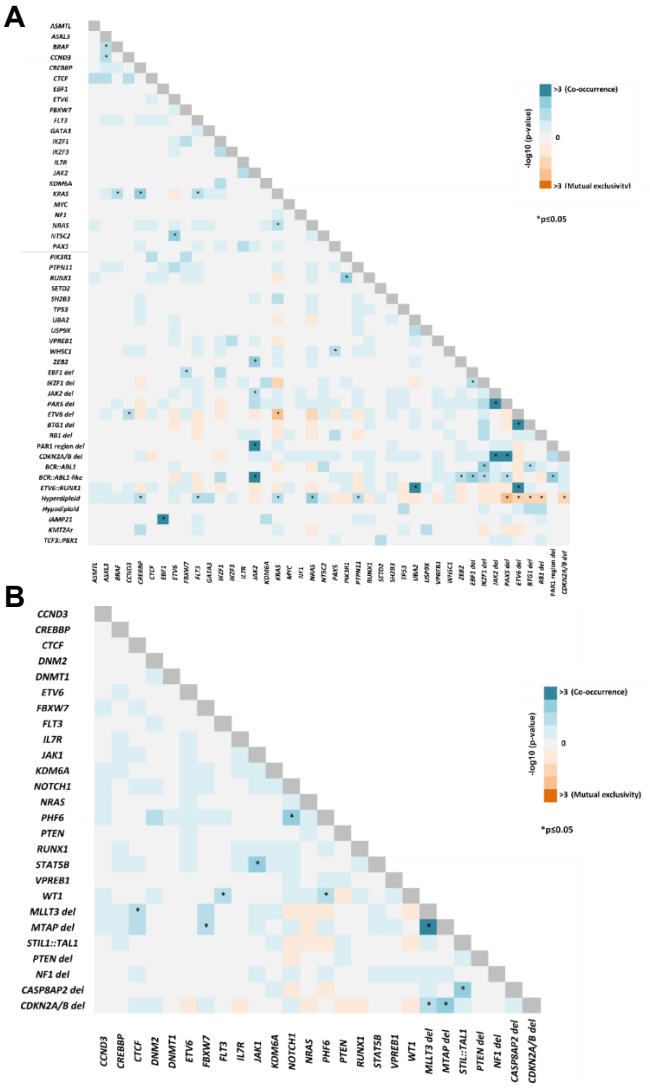

Figure 2. A Co-occurrence and mutual exclusivity of short somatic variants and subchromosomal CNAs in diagnostic samples of patients with B-ALL and **B** with T-ALL.

4.3 Genetic aberrations at relapse

Comprehensive molecular profiling was performed on paired samples of 19 patients (B-ALL: n=15, T-ALL: n=4), taken at the time of diagnosis and relapse. The average number of detected mutations was 2.4 (range: 0-5) in relapse samples, moderately surpassing the value observed in diagnostic samples (average: 2.0, range: 0-7). *NT5C2* and *CDKN2A* mutations were solely identified, and the incidence of *TP53* and *CREBBP* mutations was increased in relapse samples, both affecting 21% (4/19) of the patients. Higher variant allele frequencies at the time of relapse (VAF: 59% vs 74% and 4% vs 63%) indicated that both *TP53* mutant clones, which were present in two instances at the time of diagnosis, acquired selective survival advantage. Two patients developed *TP53* mutant clones during relapse, with one patient at the time of the second relapse, seven years after the initial diagnosis. In 13/19 patients, at least one mutation prevailed from diagnosis to relapse, the treatment eradicated additional variants in 9/19 patients, and novel alterations arose at relapse in 8/19 patients. Four patients presented with an entirely distinct mutational profile at the time of relapse. Further interrogation of the development of observed alterations over the course of the disease indicated perplexed clonal dynamics, with concurrently rising and declining subclones in two-thirds of the cases.

4.4 Genetic alterations associated with therapeutic response and prognosis

Survival analysis demonstrated significantly shorter 3-year event-free survival (EFS) in B-ALL patients with *TP53* (90% vs 50%; p=0.008. Figure 3.A) or *CREBBP* mutations (91% vs 67%; p=0.010, Figure 3.B). Strikingly, 3-year EFS of MRD negative patients on day 33 of therapy was also inferior in *TP53* mutant cases (92% vs 33%; p=0.0004, Figure 3.C).

A

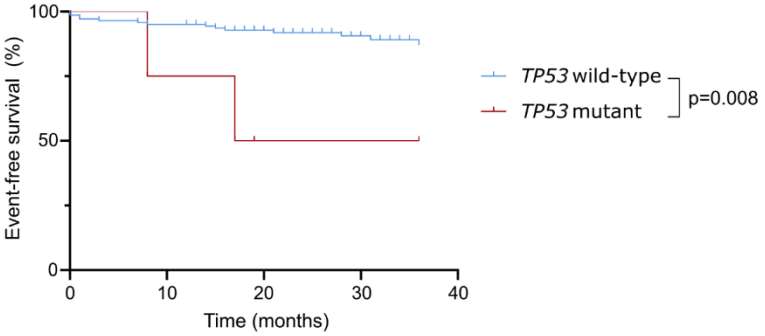
100
50
0
Event-free survival (%)
0
10
20
30
40
Time (months)
TP53 wild-type
TP53 mutant
p=0.008

B

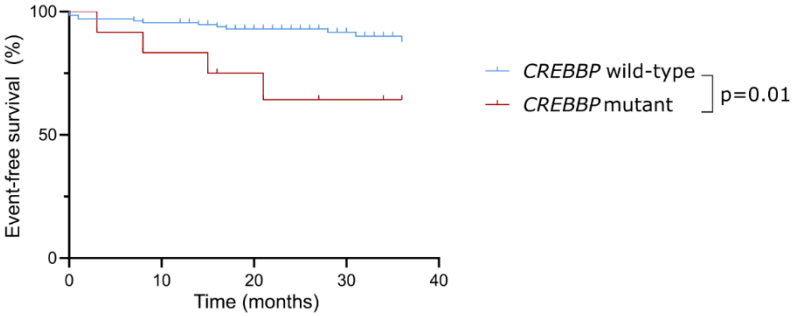
100
50
0
Event-free survival (%)
0
10
20
30
40
Time (months)
CREBBP wild-type
CREBBP mutant
p=0.01

C

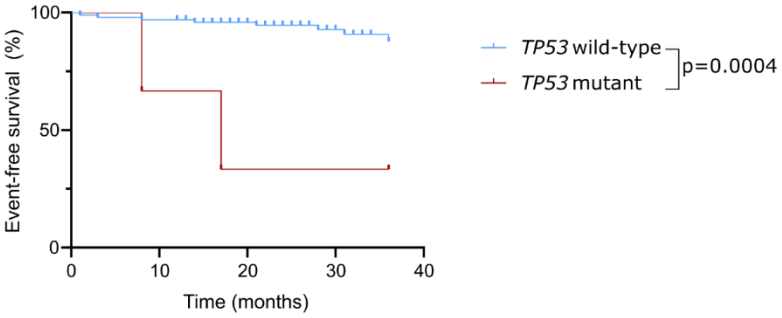
100
50
0
Event-free survival (%)
0
10
20
30
40
Time (months)
TP53 wild-type
TP53 mutant
p=0.0004

Figure 3. A Three-year event-free survival of B-ALL patients subclassified based on *TP53* mutation status. **B** Three-year event-free survival of B-ALL patients categorized based on *CREBBP* mutation status. **C** Three-year event-free survival of B-ALL patients MRD negative on day 33 and categorized based on *TP53* mutation status.

Given the limited number of patients with *TP53* and *CREBBP* mutations in our in-house cohort, we conducted a focused analysis of 3-year EFS utilizing a merged dataset comprising 411 patients, including 265 patients from the TARGET ALL Phase 2 study. Consistent with our earlier findings, survival analysis revealed poor outcomes for B-ALL patients with *TP53* or *CREBBP* mutations, even among MRD negative patients in case of *TP53* mutation in this expanded cohort (93% vs 67% p=0.0009; 93% vs 80% p=0.013; 95% vs 71% p=0.009).

Further interrogation of the subset of patients with very early or early events (EFS<24 months) uncovered that 7 out of 13 B-ALL patients were stratified to the intermediate risk (IR) arm of the ALL IC-BFM 2009 protocol and treated accordingly. Four out of these seven IR patients carried either *TP53* (n=2) or *CREBBP* (n=3) mutation. Notably, in our in-house cohort, three of the five mutations presented subclonally with a VAF of 3-5%, which range is often precarious in terms of interpretation using conventional sequencing coverage instead of deep sequencing. Mutations with a VAF ≥10%, and fusions involving putatively targetable genes, including *NRAS, KRAS, PTPN11, NF1, FLT3, JAK2, IL7R, SH2B3, CRLF2, EPOR, ABL1, ABL2, KMT2A* and *NUP98* were identified in 55.9% of ALL IC-BFM 2009 high-risk patients, and 31.6% of standard/intermediate-risk patients.

4.5 Reclassification of the level of CNS involvement based on the quantification of miR-181a-5p copy numbers

In my PhD work we also examined the copy numbers of miR-181a-5p in 92 CSF samples collected at diagnosis or different follow-up time points. Normalized copy numbers of miR-181a-5p in samples obtained at the time of diagnosis from 28 patients were used for generating a hierarchical cluster dendrogram which yielded two primary branches (Figure 4). Seven samples with ambivalent CNS status (CNSamb) and, notably, three CNSneg samples clustered together with all three CNSpos diagnostic samples. The samples in the left-hand branch were classified as 'miRsign', indicating 'significant' miR-181a-5p expression. The right-hand branch, consisting of 3 CNSamb and 12 CNSneg samples were labelled as 'miRmin', referring to minimal miR-181a-5p expression.

By integrating the miR-based CNSL classification with results of the routinely applied cellular methods, we reclassified the patients into three distinct groups indicative of initial CNS involvement: CNSneg or CNSamb samples on the right-hand branch (CNSmin & miRmin), CNSneg or CNSamb samples on the left branch (CNSmin & miRsign), and CNSpos samples (CNSpos & miRsign). The CNSneg and CNSamb samples were grouped together as the therapeutic consequence of CNS-2 category compared to CNS-1, with two additional intrathecal courses, is substantially less than the CNS-directed therapy escalation for the CNS-3 group. The two-step reclassification process is depicted in Figure 5.

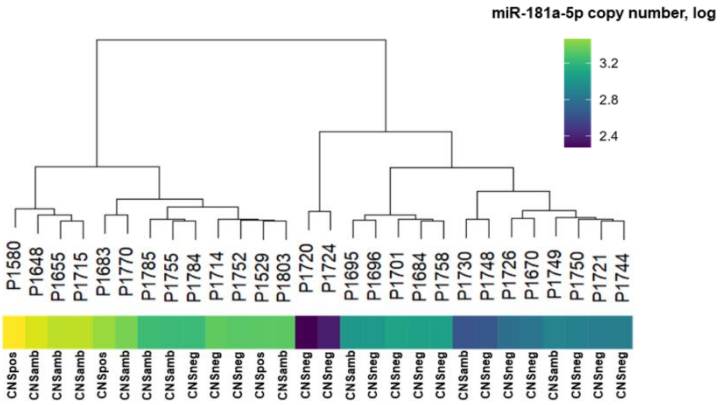

Figure 4. Dendogram, displaying the two main subgroups based on miR-181a-5p expression in the CSF, defined by hierarchical clustering. Each spike represents a patient. CNS status determined by cell-based methods is presented at the bottom.

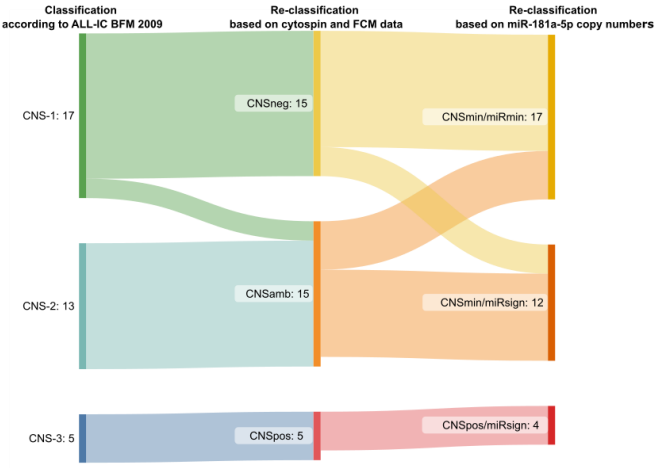

Figure 5. Sankey diagram depicting the classification of patients according to current BFM guidelines applied in clinical setting (column on the left), newly established categories used in this study and reflecting the uncertainty of cell-based methods (middle column), and a proposed re-classification, implementing miR-181a-5p expression (column on the right)

4.6 Elevated miR-181a-5p copy numbers suggest latent CNSL and aid the classification of patients with ambiguous CNS status

Using linear regression, miR-181a-5p copy numbers of samples obtained at diagnosis were compared. Higher levels of miR-181a-5p were found in the CNSmin/miRsign group and the CNSpos/miRsign group, as opposed to the CNSmin/miRmin group (mean copy number ± standard error (SE): 2503.50±275.89, 3300.70±809.69 and 744.02±86.81, respectively; p=1.13E-6 and p=2.16E-5 when comparing miRsign groups to CNSmin/miRmin group) (Figure 6.A). Patients with FCM positivity exhibited significantly elevated miR-181a-5p expression relative to those with negative CSF analysis by FCM (p=0.016; Figure 6.B).

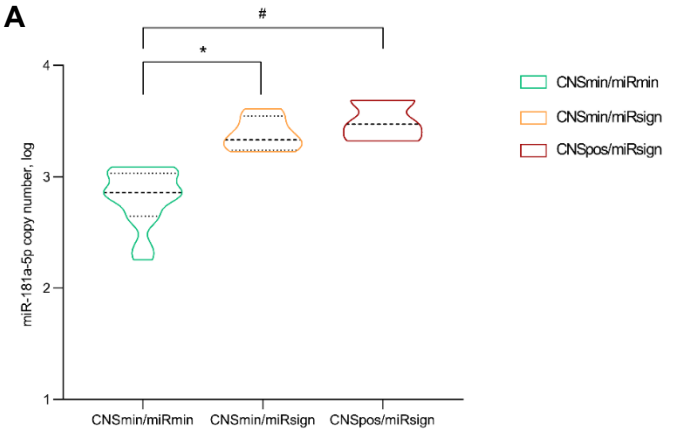

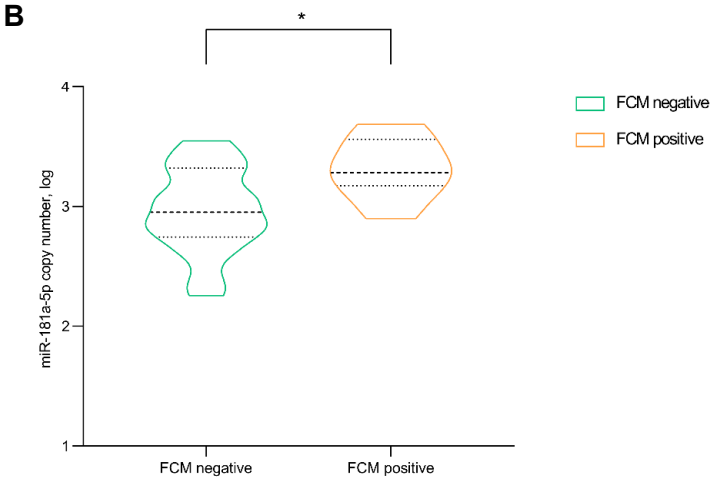

Figure 6. A Violin plot displaying the distribution of the logarithm of miR181-a-5p copy numbers of CSF samples collected at the time of diagnosis, measured by ddPCR. * p=1.13E-6; # p=2.16E-5 **B** Violin plot illustrating the distribution of the logarithm of miR181-a-5p copy numbers of CSF samples collected at the time of diagnosis in patients with either negative or positive CSF flow cytometry. * p=0.016.

4.7 Diagnostic value of ddPCR-based miR-181a-5p quantification

To evaluate the diagnostic value of miR-181a-5p copy number assessment by ddPCR, ROC analysis was conducted, comparing the feasibility of the novel biomarker with cell-based techniques, such as cytospin and FCM. A cut-off value for miR-181a-5p copies was determined statistically, and as a result, copy numbers above 1,454 copies were considered positive in the consecutive binary transformation. Analysis of the curves indicated that our innovative miR-181a-5p copy number-based

methodology outperformed cytospin and was non-inferior to FCM.

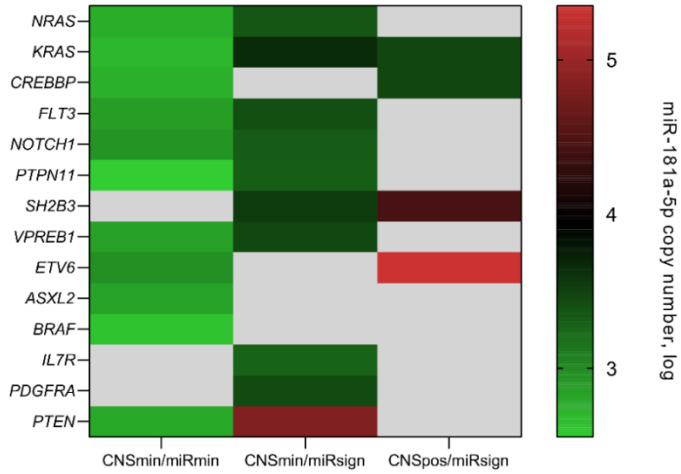

Figure 7. Heatmap, displaying the logarithm of miR-181a-5p copy numbers and genes altered in a minimum of two patients, illustrated by groups. Grey shaded fields indicate no mutation in the gene of interest identified in the respective groups. The mean logarithm of miR-181a-5p copy number is presented for genes altered in several patients within a certain field.

4.8 *SH2B3* alteration identified as CNSL-associated genetic feature

We also investigated the possible relations between miR-181a-5p copy numbers and small sequence variations (single nucleotide variants and small insertions/deletions) in disease-relevant genes detected in blast-rich BM samples. Twelve out of the 103 leukemia-relevant genes were mutated in at least 2 patients (Figure 7). Strikingly, *SH2B3* mutations solely affected patients classified in miRsign groups (CNSmin/miRsign or

CNSpos/miRsign), with no *SH2B3* mutation found in the miRmin group.

5. CONCLUSIONS

Novel findings of my thesis are the following:

- We present a systematic comprehensive molecular profiling approach as part of the diagnostic workflow in a nationwide consecutive cohort of children with ALL.
- We demonstrated that targeted RNA-seq complemented by (digital)MLPA is a powerful method for identifying recently introduced genetic subtypes of ALL and offers a viable alternative to existing diagnostic techniques.
- We conducted mutational screening using targeted deep DNA-seq and detected small genomic variants in ALL, even if those were present with a low variant allele frequency, which may have clinical relevance, as exemplified in other hematological malignancies.
- We observed inferior outcome among B-ALL patients harboring *TP53* or *CREBBP* mutation.
- We found shorter event-free survival in *TP53* mutant B-ALL patients, even among those testing negative for MRD by flow cytometry on day 33 of therapy.
- We compared the genomic profile of matched diagnostic and relapse samples of 19 ALL patients and shed light to the manifold evolutionary process and entangled clonal selection mechanisms.
- We propose miR-181a-5p as a novel biomarker in the cerebrospinal fluid for the diagnosis of CNSL and demonstrate a feasible quantification method by ddPCR.
- We tested the diagnostic power of miR-181a-5p quantification by ddPCR, and found that it is non-inferior to FCM, and overperforms cytospin in identifying CNSL.
- We discovered an association between *SH2B3* mutations and miR-181a-5p expression, indicating a potential role of *SH2B3* mutations in the leukemic invasion of CNS.

6. BIBLIOGRAPHY OF THE CANDIDATE'S PUBLICATIONS

Publications related to the PhD Thesis:

1. Péterffy, Borbála ; Nádasi, Tamás János ; Krizsán, Szilvia ; Horváth, Anna ; Márk, Ágnes ; Barna, Gábor ; Timár, Botond ; Almási, Laura ; Müller, Judit ; Csanádi, Krisztina ; Rakonczai, Anna ; Nagy, Zsolt ; Kállay, Krisztián ; Kertész, Gabriella ; Kriván, Gergely ; Csóka, Monika ; Sebestyén, Anna ; Semsei, Ágnes ; Kovács, Gábor Tamás ; Erdélyi, Dániel János ; Bödör, Csaba ; Egyed, Bálint* ; Alpár, Donát*.
Digital PCR-based quantification of miR-181a in the cerebrospinal fluid aids patient stratification in pediatric acute lymphoblastic leukemia
SCIENTIFIC REPORTS 14 : 1 Paper: 28556 , 13 p. (2024); * joint senior authors

2. Péterffy, Borbála ; Krizsán, Szilvia ; Egyed, Bálint ; Bedics, Gábor ; Benard-Slagter, Anne ; Palit, Sander ; Erdélyi, Dániel János ; Müller, Judit ; Nagy, Tibor ; Hegyi, Lajos László ; Bekő, Anna ; Kenéz, Lili Anna ; Jakab, Zsuzsanna ; Péter, György ; Zombori, Marianna ; Csanádi, Krisztina ; Ottóffy, Gábor ; Csernus, Katalin ; Vojcek, Ágnes ; Tiszlavicz, Lilla Györgyi ; Gábor, Krisztina Míta ; Kelemen, Ágnes ; Hauser, Péter; Kállay, Krisztián ; Kertész, Gabriella ; Gaál, Zsuzsanna ; Szegedi, István ; Barna, Gábor ; Márk, Ágnes ; Haltrich, Irén ; Hevessy, Zsuzsanna ; Ujfalusi, Anikó ; Kajtár, Béla ; Timár, Botond ; Kiss, Csongor ; Kriván, Gergely ; Matolcsy, András ; Savola, Suvi ; Kovács, Gábor ; Bödör, Csaba ; Alpár, Donát.
Molecular profiling reveals novel gene fusions and genetic markers for refined patient stratification in pediatric acute lymphoblastic leukemia
MODERN PATHOLOGY 38 : 6 Paper: 100741 , 14 p. (2025); * joint senior authors

Other publications:

1. Török, Marianna; Merkely, Petra ; Monori-Kiss, Anna ; Horváth, Eszter Mária ; Sziva, Réka Eszter ; Péterffy, Borbála ; Jósvai, Attila ; Sayour, Alex Ali ; Oláh, Attila ; Radovits, Tamás ; Merkely, Béla ; Ács, Nándor ; Nádasy György László ; Várbíró, Szabolcs.

Network analysis of the left anterior descending coronary arteries in swim-trained rats by an in situ video microscopic technique
BIOLOGY OF SEX DIFFERENCES 12 : 1 Paper: 37 , 17 p. (2021)

2. Tarszabó, Róbert ; Bányai, Bálint ; Ruisanchez, Éva ; Péterffy, Borbála ; Korsós-Novák, Ágnes ; Lajtai, Krisztina ; Sziva, Réka Eszter ; Gerszi, Dóra ; Hosszú, Ádám ; Benkő, Rita ; Benyó, Zoltán ; Horváth, Eszter Mária ; Masszi, Gabriella ; Várbíró, Szabolcs.
Influence of Vitamin D on the Vasoactive Effect of Estradiol in a Rat Model of Polycystic Ovary Syndrome
INTERNATIONAL JOURNAL OF MOLECULAR SCIENCES 22 : 17 Paper: 9404 , 12 p. (2021)

3. Sipos, Miklós ; Péterffy, Borbála ; Sziva, Réka Eszter ; Magyar, Péter ; Hadjadj, Leila ; Bányai, Bálint ; Süli, Anita ; Soltész-Katona, Eszter ; Gerszi, Dóra ; Kiss, Judit ; Szekeres, Mária ; Nádasy, György László; Horváth, Eszter Mária ; Várbíró, Szabolcs.
Vitamin D Deficiency Cause Gender Specific Alterations of Renal Arterial Function in a Rodent Model
NUTRIENTS 13 : 2 Paper: 704 , 13 p. (2021)

4. Lajtai, Krisztina ; Tarszabó, Róbert ; Bányai, Bálint ; Péterffy, Borbála ; Gerszi, Dóra ; Ruisanchez, Éva ; Sziva, Réka Eszter ; Korsós-Novák, Ágnes ; Benkő, Rita ; Hadjadj, Leila ; Benyó, Zoltán ; Horváth, Eszter Mária ; Masszi, Gabriella ; Várbíró, Szabolcs.
Effect of Vitamin D Status on Vascular Function of the Aorta in a Rat Model of PCOS
OXIDATIVE MEDICINE AND CELLULAR LONGEVITY 2021 Paper: 8865979 , 6 p. (2021)

5. Hannah, Armes ; Ana, Rio-Machin ; Krizsán, Szilvia ; Bödör, Csaba ; Fadimana, Kaya ; Findlay, Bewicke-Copley ; Jenna, Alnajar ; Amanda, Walne ; Péterffy, Borbála ; Hemanth, Tummala ; Rouault-Pierre, Kevin ; Dokal, Inderjeet ; Vulliamy , Tom ; Fitzgibbon, Jude.
Acquired somatic variants in inherited myeloid malignancies
LEUKEMIA 36 : 5 pp. 1377-1381. , 5 p. (2022)

6. Krizsán, Szilvia ; Péterffy, Borbála ; Egyed, Bálint ; Nagy, Tibor ; Sebestyén, Endre ; Hegyi, Lajos László ; Jakab, Zsuzsanna ; Erdélyi, Dániel J. ; Müller, Judit ; Péter, György ; Csanádi, Krisztina ; Kállay, Krisztián ; Kriván, Gergely ; Barna, Gábor ; Bedics, Gábor ; Haltrich, Irén ; Ottóffy, Gábor ; Csernus, Katalin ; Vojcek, Ágnes ; Tiszlavicz, Lilla Györgyu ; Gábor, Krisztina Mita, Kelemen, Ágnes ; Hauser, Péter ; Gaál, Zsuzsanna ; Szegedi, István ; Ujfalusi, Anikó ; Kajtár, Béla ; Kiss, Csongor ; Matolcsy, András ; Timár, Botond ; Kovács, Gábor ; Alpár, Donát ; Bödör, Csaba.
Next-Generation Sequencing–Based Genomic Profiling of Children with Acute Myeloid Leukemia
JOURNAL OF MOLECULAR DIAGNOSTICS 25 : 8 pp. 555-568. , 14 p. (2023)

7. Hunyadi, Anna ; Kriston, Csilla ; Szalóki, Gabor ; Péterffy, Borbála ; Egyed, Bálint ; Szepesi, Ágota ; Timár, Botond ; Erdélyi, Dániel János ; Csanádi, Krisztina ; Kutszegi, Nóra ; Márk, Ágnes ; Barna, Gábor.
The significance of CD49f expression in pediatric B-cell acute lymphoblastic leukemia
AMERICAN JOURNAL OF CLINICAL PATHOLOGY 163 : 2 pp. 169-177. , 9 p. (2025)

8. Egyed, Bálint ✉ ; Árvai, Kristóf ; Zajta, Erik ; Hegyi, Lajos ; Andrássy, Blanka ; Kovács, Árpád Ferenc ; Bekő, Anna ; Péterffy, Borbála ; Erdélyi, Dániel János ; Müller, Judit ; Békési, Andrea ; Kállay, Krisztián ; Goda, Vera ; Kriván, Gergely ; Tuboly, Eszter ; Csanádi, Krisztina ; Ottóffy, Gábor ; Szegedi, István ; Kiss, Csongor ; Bödör, Csaba ; Alpár, Donát ; Kovács, Gábor.
A genetikai eredetű gyermekkori krónikus cytopeniák felismerése a molekuláris medicina érájában : Klinikai ajánlás és metodikai útmutató
ORVOSI HETILAP 166 : 1 pp. 3-19. , 17 p. (2025)